A&A 644, A63 (2020)
https://doi.org/10.1051/0004-6361/202038997

Astronomy & Astrophysics

Optical spectroscopy of 4U 1812–12

An ultra-compact X-ray binary seen through an H II region

M. Armas Padilla[1,2], T. Muñoz-Darias[1,2], F. Jiménez-Ibarra[1,2], J. A. Fernández-Ontiveros[3], J. Casares[1,2], M. A. P. Torres[1,2], J. García-Rojas[1,2], V. A. Cúneo[1,2], and N. Degenaar[4]

[1] Instituto de Astrofísica de Canarias (IAC), Vía Láctea s/n, La Laguna 38205, S/C de Tenerife Spain
e-mail: m.armaspadilla@iac.es
[2] Departamento de Astrofísica, Universidad de La Laguna, La Laguna 38205, S/C de Tenerife, Spain
[3] Istituto di Astrofisica e Planetologia Spaziali (INAF–IAPS), Via Fosso del Cavaliere 100, 00133 Roma, Italy
[4] Anton Pannekoek Institute for Astronomy, University of Amsterdam, Science Park 904, 1098 XH Amsterdam, The Netherlands

Received 22 July 2020 / Accepted 14 September 2020

ABSTRACT

The persistent low-luminosity neutron star X-ray binary 4U 1812−12 is a potential member of the scarce family of ultra-compact systems. We performed deep photometric and spectroscopic optical observations with the 10.4 m Gran Telescopio Canarias in order to investigate the chemical composition of the accreted plasma, which is a proxy for the donor star class. We detect a faint optical counterpart ($g \sim 25$, $r \sim 23$) that is located in the background of the outskirts of the Sharpless 54 H II region, whose characteristic nebular lines superimpose on the X-ray binary spectrum. Once this is corrected for, the actual source spectrum lacks hydrogen spectral features. In particular, the Hα emission line is not detected, with an upper limit (3σ) on the equivalent width of <1.3 Å. Helium (He I) lines are also not observed, even though our constraints are not restrictive enough to properly test the presence of this element. We also provide stringent upper limits on the presence of emission lines from other elements, such as C and O, which are typically found in ultra-compact systems with C−O white dwarfs donors. The absence of hydrogen features, the persistent nature of the source at low luminosity, and the low optical–to–X-ray flux ratio confirm 4U 1812−12 as a compelling ultra-compact X-ray binary candidate, for which we tentatively propose a He-rich donor based on the optical spectrum and the detection of short thermonuclear X-ray bursts. In this framework, we discuss the possible orbital period of the system according to disc instability and evolutionary models.

Key words. accretion, accretion disks – stars: neutron – X-rays: binaries – X-rays: individuals: 4U 1812–12

1. Introduction

Ultra-compact X-ray binaries are systems of great interest for a number of reasons (e.g. stellar and binary evolution, gravitational wave detection, thermonuclear burning; Nelemans et al. 2009; Tauris 2018). These X-ray binaries, which so far have been found to harbour neutron star accretors, are tight in orbital periods shorter than ∼80 min where only a degenerate companion, such as a He star or white dwarf, can fit within the small Roche lobe (Rappaport et al. 1982). The current population of ultra-compact X-ray binaries comprises 14 systems (with reported orbital periods; see e.g. Heinke et al. 2013, and references therein; Strohmayer et al. 2018), even though $\sim 10^5$ of these sources are predicted to be hosted in our Galaxy (Van Haaften et al. 2013). We might be missing large numbers of these systems because of the observational challenges in measuring orbital periods of low-mass X-ray binaries (LMXBs; Casares et al. 2017) in general, and the faintness of these systems in particular. Some indirect evidence used to identify ultra-compact candidates is based on their X-ray faintness, a direct consequence of their small accretion discs. According to the disc instability model, systems persistently accreting at very low X-ray luminosities should have short orbital periods since smaller discs can be entirely ionised at lower accretion rates (Lasota 2001; in 't Zand et al. 2007). Thus, ultra-compact systems could sustain a persistent behaviour when accreting at $L_X \lesssim 10^{36}$ erg s^{-1}, while systems with longer orbits have persistent X-ray luminosities of $\sim 10^{37-38}$ erg s^{-1} (see e.g. Nelemans & Jonker 2010; Revnivtsev et al. 2012). Likewise, small accretion discs result in lower optical–to–X-ray flux ratios because the disc region responsible for the X-ray (to optical) reprocessing is also smaller (van Paradijs & McClintock 1994). Additional (also indirect) diagnostics are based on the degenerate nature of the donor star. These rely on the absence or presence of emission and absorption features in the source spectra, which provide hints on the chemical composition of the accreted material, and thus, on the nature of the companion star. We refer to Nelemans et al. (2004), Baglio et al. (2016), and Hernández Santisteban et al. (2019) for examples of optical studies; Homer et al. (2002) and Tudor et al. (2018) of UV studies; and Juett & Chakrabarty (2003), Schulz et al. (2001), and Armas Padilla & López-Navas (2019), among others, for studies at X-ray energies.

The X-ray binary 4U 1812−12 fulfils several of the above distinctive features. Since its discovery by the Uhuru mission (Forman et al. 1976), the source has consistently displayed a low (unabsorbed) X-ray flux of a few times 10^{-10} erg cm^{-2} s^{-1} (e.g. Warwick et al. 1981; Wilson et al. 2003; Barret et al. 2003; Muno et al. 2005). Numerous type I bursts have been reported, unveiling the neutron star nature of the compact object (e.g. Murakami et al. 1983; Tarana et al. 2006). Many of these bursts show photospheric radius expansion that, assuming Eddington-limited

luminosities, place the source at ~3.4–4.6 kpc (Cocchi et al. 2000; Jonker & Nelemans 2004). This implies a persistent X-ray luminosity of $\sim 10^{36}$ erg s^{-1} (~1% of the Eddington luminosity ($L_{\rm Edd}$)). In the same way, the $R = 22.15$ optical counterpart corresponds to an absolute magnitude of ~3.6–4.2 (Bassa et al. 2006). Thus, both the persistently low X-ray luminosity and the low optical–to–X-ray flux ratio make 4U 1812−12 a promising ultra-compact X-ray binary candidate (Bassa et al. 2006; in 't Zand et al. 2007).

In order to investigate further whether 4U 1812−12 belongs to the ultra-compact class, we obtained deep optical spectroscopy and Hα imaging with the 10.4 m Gran Telescopio Canarias (GTC). Here, we present the results of this campaign, including the identification of an extended nebula in the sky region surrounding the system.

2. Observations and data reduction

We observed 4U 1812−12 on 2018 June 13 with the Optical System for Imaging and low-Intermediate Resolution Integrated Spectroscopy (OSIRIS; Cepa et al. 2000) attached to the GTC at the Observatorio del Roque de Los Muchachos in La Palma, Spain. We used the grism R1000R (2.62 Å pix^{-1}), which covers the spectral range 5100−10 000 Å. We took four spectra of 1400 s each using a slit-width of 1 arcsec, which provided a spectral resolution of 474 ± 3 km s^{-1} (measured as the full width at half-maximum of a sky line at ~6300 Å). We reduced and combined the data using IRAF[1] tools and custom PYTHON routines, whereas the package MOLLY[2] was used for the analysis.

In addition, we obtained narrow-band GTC/OSIRIS photometry (3 × 900 s) of the field (2019 August 1) using the SHARDS filter U653/17, which is centred at 6530 Å (i.e. close to Hα) and has a bandpass of 160 Å. We also took 120 s images using the filters SDSS-g and SDSS-r for photometric measurements. Data were reduced using ASTROPY-CCDPROC routines (Robitaille et al. 2013; Price-Whelan et al. 2018; Craig et al. 2017).

3. Analysis and results

Aperture photometry of the SDSS-g and SDSS-r images was carried out using PHOTUTILS (Bradley et al. 2019) and calibrated against field stars in the PanSTARRS catalogue (Chambers et al. 2016). The optical counterpart of 4U 1812−12 is detected in both exposures, even though it is significantly fainter in the blue filter ($g = 25.3 \pm 0.3$) than in the red band ($r = 22.76 \pm 0.07$). The latter is broadly consistent with $R = 22.15$ reported in Bassa et al. (2006). This indicates that the source is significantly absorbed, in agreement with the value of $N_{\rm H} \sim 1.5 \times 10^{22}$ cm^{-2} derived in Tarana et al. (2006). Using the standard $N_{\rm H}$–A_v relation in Predehl & Schmitt (1995) and the prescription of Yuan et al. (2013) to calculate reddening coefficients, this $N_{\rm H}$ translates into $A_g \sim 9$ mag and $A_r \sim 6.2$ mag. This is fairly consistent with the magnitudes reported above.

The trace of 4U 1812−12 was clearly detected in the four spectra redward of 5700 Å, which together with the strong telluric features present in the red part of the spectrum restrict our analysis to the spectral range 5700−7500 Å. The 2D spectra reveal the presence of extended emission in the Hα spectral region. A careful extraction using background regions not contaminated by this extended emission (labelled "A"; middle panel in Fig. 1), shows a strong and narrow Hα line accompanied by [N II] λ6548, 6584, as well as weaker [S II] λ6717, 6731 emission (see red spectrum in the bottom panel of Fig. 1). Unlike Hα, these forbidden transitions are not characteristic of LMXBs. A close look at the spatial profile of our spectra along the slit reveals that the lines arise in an asymmetric extended region around the source (see middle panel in Fig. 1). The most intense emission region has a size of ~35 arcsec (~25 arcsec from the source position to the north and ~10 arcsec to the south), although it expands further with a dimmer intensity. In a second step, we performed additional extractions considering background regions progressively closer to the trace of the target. As expected, this made the nebular emission weaker, and eventually disappear. The bottom panel of Fig. 1 shows the average spectrum obtained by considering the background regions labelled "B" in the middle panel. These were chosen to minimise the presence of nebular [N II] features in the final spectrum. This also makes Hα disappear (see Sect. 3.2). As can be seen in Fig. 1 (bottom panel) the two extractions, using sky regions A and B, yield remarkably similar continuum levels, with the exception of the spectral regions including the above-mentioned nebular lines. This is consistent with the spectrum drawn in red being the sum of that of 4U 1812−12 (i.e. the black one) and the contribution of a nebula in some characteristic transitions. For a more meaningful representation, both spectra were flux calibrated against the flux standard GD140 that was observed at the end of the night.

The narrow-band imaging, top panel in Fig. 1, shows that 4U 1812−12 is located in the outskirts of a region with a high density of diffuse gas. Indeed, the intensity profile of our 2D spectrum (middle panel) matches the nebular structure covered by the slit in the spatial direction (top right panel).

3.1. Origin of the nebular emission

There is a variety of astrophysical objects, such as H II regions, planetary nebulae, and supernova remnants, that naturally produce the nebular features that we have observed. In addition, some X-ray binaries have been associated with nebular structures produced by either photo-ionisation by high-energy radiation (e.g. Cooke et al. 2007, 2008) or shock-ionisation due to the impact of the binary jet on the interstellar medium (e.g. Russell et al. 2007; Wiersema et al. 2009).

In order to distinguish whether the surrounding diffuse emission is related to 4U 1812−12, we investigated some characteristic emission line ratios commonly used as diagnostics of shock-ionised or photo-ionised gas. In particular, we use the Sabbadin & D'Odorico (1976) diagnostic diagram, which uses the spectral lines that are more prominent in our spectra (Hα/[N II] versus Hα/[S II]). We obtain Hα/[N II]$_{(6548+6584)}$ = 1.7 ± 0.1 and Hα/[S II]$_{(6717+6731)}$ = 4.1 ± 0.4, values that comfortably lie in the zone occupied by H II regions (see Fig. 10 in Öttl et al. 2014; see also Magrini et al. 2003). Exploring the location of our source, we tentatively identify the diffuse gas surrounding 4U 1812−12 as being part of the large H II emission nebula Sharpless 54 (Sh2-54) placed eastward from the target. This region is ionised by the open cluster NGC 6604, located in the Serpens constellation, at ~1.5 kpc (Zucker et al. 2020; see Fig. 1). Thus, the nebular emission is most likely in the foreground of 4U 1812−12, which is located at ~4 kpc from the Earth.

[1] IRAF, the Image Reduction and Analysis Facility, is distributed by the National Optical Astronomy Observatory, which is operated by the Association of Universities for Research in Astronomy under cooperative agreement with the National Science Foundation.

[2] http://deneb.astro.warwick.ac.uk/phsaap/software/molly/html/INDEX.html

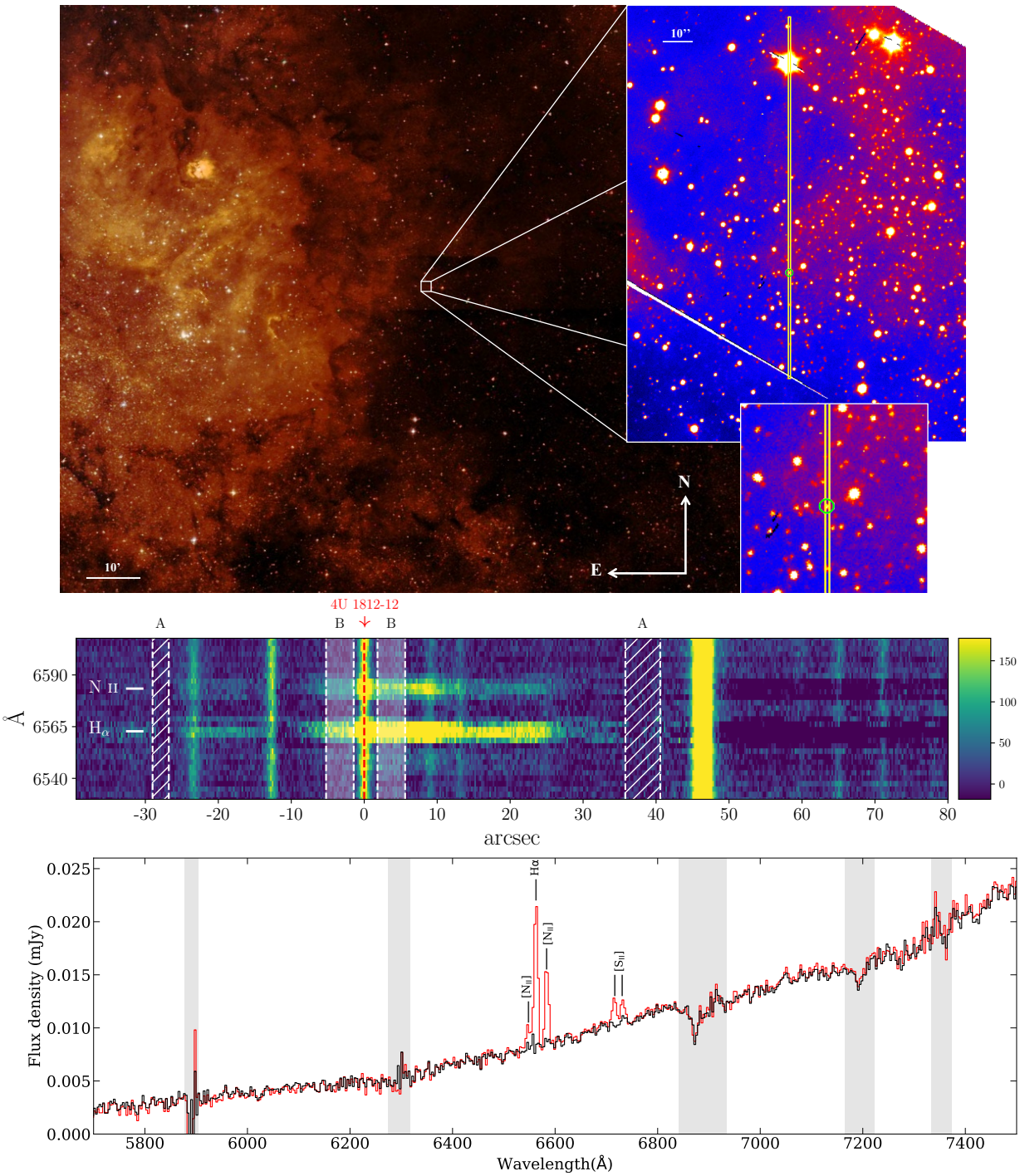

Fig. 1. *Top panel*: DSS2 coloured image of $2^\circ \times 1.8^\circ$ including 4U 1812−12 (white rectangle), which is located in the outskirts of the H II nebula Sharpless 54. A zoom-in on the target region using our Hα narrow-band imaging is shown together with the position of the slit in the spectroscopic data. A 120 arcsec region covered by the slit along the spatial axis and corresponding to the 2D spectrum (*middle panel*) is represented by a yellow rectangle, while the position of the system is indicated by a green circle. For better visualization, the closest region to the target is magnified further. *Middle panel*: zoom-in on 2D spectrum in the Hα region, covering 120 arcsec in the spatial direction. The position of 4U 1812−12 is indicated by a dashed red line. The vertical white stripes denote the different background regions considered for the overall (A) and nebula-free (B) spectra (see text). Intensity is indicated by a colour scale from 0 (deep blue) to 160 (bright yellow) counts. *Bottom panel*: average spectra obtained by considering the A (red) and B (black) background regions. The grey-shaded bands indicate spectral regions affected by interstellar or telluric features.

3.2. Optical spectrum of 4U 1812−12

We inspected the spectrum of 4U 1812−12 searching for features indicative of the chemical composition of the accreted material, and thus of the nature of the companion star. Neither H nor He emission lines are detected (see Fig. 2). In Table 1 we list the 3σ upper limits on the equivalent width (EW) of Hα and some He I lines, which are characteristic of LMXBs with H-rich companion stars (e.g. Charles & Coe 2006; Mata Sánchez et al. 2018). These were calculated using 1500 km s^{-1} wide spectral regions, which

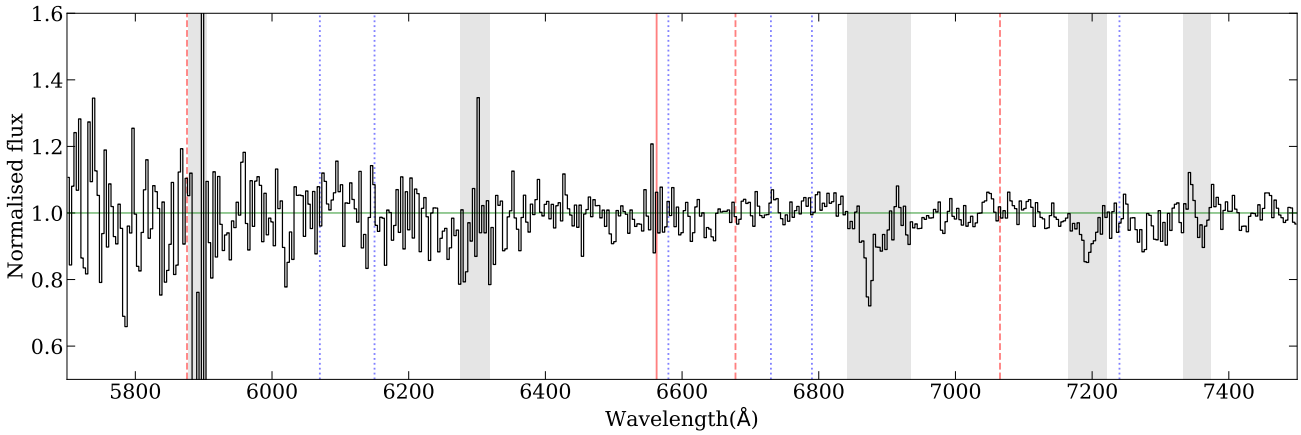

Fig. 2. Normalised spectrum of 4U 1812−12 after subtraction of the nebular contribution (i.e. using the B-labelled regions from Fig. 1 for background correction). The red vertical lines indicate the position of Hα (solid) and several He emission lines (dashed). The vertical dotted blue lines indicate the approximate location of C and O blends detected in some ultra-compact systems (Nelemans et al. 2004). The grey-shaded bands indicate the spectral regions affected by interstellar or telluric features.

Table 1. Upper limits (3σ) on the EW of some of the most prominent lines of classic LMXBs (i.e. with H-rich donors) and C−O blends detected in ultra-compact X-ray binaries (see Nelemans et al. 2004).

Line	λ_c (Å)	EW (Å)
He I	5875.6	<2.8
Hα	6562.8	<1.3
He I	6678.1	<1.1
He I	7065.2	<0.9
Blend	**Spectral range [(a)] (Å)**	**EW (Å)**
C II	6040–6120	<4.6
C II–C III	6130–6180	<3.3
C II–O II	6550–6600	<1.5
C III–O II	6700–6760	<1.3
C II–C III	6760–6820	<1.3
C II	7210–7260	<1.1

Notes. [(a)]EWs calculated in the spectral ranges used in Nelemans et al. (2004).

is a standard value for the full width at half maximum of Hα in LMXBs (Casares 2015), centred at the rest wavelength of each transition.

Similarly, we also investigated the presence of C and O features, which have been detected in the optical spectra of some (candidate) ultra-compact X-ray binaries favouring C−O white dwarf companions (see e.g. Nelemans et al. 2004; Werner et al. 2006). None of these features are significantly detected (3σ) in our spectra (see Table 1 for upper limits on the EW for the most prominent blends of C and O lines Nelemans et al. 2004; in 't Zand et al. 2008).

4. Discussion

The neutron star X-ray binary 4U 1812−12 has been recursively detected at $\sim 10^{36}$ erg s^{-1} in every X-ray observation performed since its discovery 50 years ago. This persistent activity at low luminosity guided in 't Zand et al. (2007) to propose an ultra-compact orbit for the source. Likewise, Bassa et al. (2006) suggested a short orbital period on the basis of the low optical–to–X-ray flux ratio (van Paradijs & McClintock 1994). Here, we reported on deep, optical spectroscopy aiming to identifying the companion star class and further test the ultra-compact nature of the system.

Our narrow-band imaging shows that 4U 1812−12 is located in a patch of the sky with a high density of diffuse gas. The optical spectrum revealed conspicuous Hα, [N II], and [S II] emission lines, similar to those typically found in H II regions. The flux ratios derived from these features strongly support this association. Thus, we tentatively identify this diffuse gas region surronding the target as being part of the nearby H II nebula Sharpless 54 located at ~1.5 kpc (Zucker et al. 2020) in the Serpens constellation. Considering the distance of ~4 kpc inferred from the detection of Eddington-limited thermonuclear bursts, we conclude that the nebular emission is in the foreground of 4U 1812−12, and therefore that both astrophysical objects are unrelated.

Once the nebular contribution is subtracted (see Sect. 3), the spectrum of 4U 1812−12 lacks any of the strong H and He features typically found in LMXBs, supporting the ultra-compact nature proposed for the system. On the one hand, in classic LMXBs (i.e. with H-rich, low-mass companion stars) Hα is typically the most prominent optical emission line. Its EW is anti-correlated with the continuum luminosity (X-ray and optical), with typical values of EW > 10 Å for X-ray luminosities $L_X \lesssim 10^{36}$ erg s^{-1} (Fender et al. 2009). This is significantly higher than our ~1.3 Å upper limit. On the other hand, He I features are much weaker in LMXBs, with He I at 5876 Å being typically the strongest line. Unfortunately, this transition is in the blue part of our spectral range, where the signal-to-noise ratio (S/N) is poorer. Thus, our upper limit on the EW (<2.8 Å) is not particularly constraining. Likewise, our more stringent upper limits on the redder He I transitions do not rule out the presence of He in the accretion disc. Indeed, theoretical modelling of hot discs in ultra-compact systems favour the formation of He II lines above those of He I (Werner et al. 2006). This is consistent with the modelling by Nelemans et al. (2006), which predict the presence of strong He II λ4686 and weaker He I λ5876, with the remaining He transitions being too weak to be detected unless very high S/N data are achieved. Our deep photometry ($g \sim 25$) indicates that testing the presence of He II λ4686 in the spectrum of 4U 1812−12 will not be feasible in the near future.

A number of confirmed ultra-compact systems also show featureless optical spectra. Deep Gemini spectroscopy of the

~38 min orbital period LMXB IGR J17062−6143 (Strohmayer et al. 2018) reveal a blue continuum with no emission lines (Hernández Santisteban et al. 2019). In addition, the ultra-compact system 2S 0918−549 ($P_{\rm orb}$ = 17.4 min, Zhong & Wang 2011) and the candidate A 1246−58 do not show significant features in Very Large Telescope spectra (Nelemans et al. 2004; Nelemans & Jonker 2010; in 't Zand et al. 2008). However, some ultra-compact systems did show emission lines of elements other than H. In particular, the detection of C and O emission features in the optical spectra of 4U 0614+091, 4U 1626−67 and 4U 1543−624 evidences the presence of metal-rich material in the accretion disc, suggesting a C–O white dwarf donor for these sources (Nelemans et al. 2004, 2006; Werner et al. 2006; Baglio et al. 2014). These emission lines are not present in our GTC spectrum. In particular, for the C−O blends between 6500 and 7300 Å we derive 3σ upper limits (<1.1−1.5 Å), which are significantly smaller than the 1.5−4 Å EWs reported in the above-mentioned works. Likewise, the presence of He II and N III emission lines in the spectrum of the dipper system 4U 1916−05 provided the first direct evidence of a He-rich companion star in an ultra-compact X-ray binary (Nelemans et al. 2006). This scenario is supported by the detection of frequent short bursts episodes, which in this case would be ignited by pure (or almost pure) He accreted fuel (see e.g. Galloway et al. 2008). Finally, we also note that the transient ultra-compact candidate 1RXS J180408.9−342058 (Baglio et al. 2016; Degenaar et al. 2016) shows a hint of He II emission at 4686 Å. Based on this, Baglio et al. (2016) proposed a He white dwarf companion in a ~40 min orbit.

The properties of thermonuclear X-ray bursts, such as duration, recurrence time and radiated energy, provide hints on the composition of the accreted fuel. As a rule of thumb, regular short ($\lesssim$1 min) X-ray bursts are fuelled by He or a mixture of H and He, while intermediate and long bursts (several minutes to hours) are powered by He and C burning, respectively (see e.g. Cumming 2003; Falanga et al. 2008; Galloway et al. 2010). In this regard, 4U 1812−12 has displayed numerous regular bursts (Murakami et al. 1983; Cocchi et al. 2000; Tarana et al. 2006; Galloway et al. 2020). Assuming the premise of the ultra-compact nature, these would be fuelled by pure He, pointing therefore to a He-rich donor, similarly to 4U 1916−05. Interestingly, the properties of 4U 1812−12 resemble to some extent those displayed by 4U 1916−05: a persistent X-ray luminosity of ~0.01 $L_{\rm Edd}$, a low optical–to–X-ray luminosity ratio, the above-mentioned episodes of short thermonuclear bursts and the lack of H lines in the optical spectra. As discussed above, the faintness of the source in the blue ($g \sim 25$) prevented us from testing the presence of the distinctive He II–N III lines observed in 4U 1916−05, which are located at 4000−5000 Å (Nelemans et al. 2006). Therefore, we cannot rule out that a similar scenario might apply to 4U 1812−12.

This would not be in conflict with the disc instability model for He accretion discs. Following Coriat et al. (2012) we derive[3] a persistent mass transfer rate of $\sim 5 \times 10^{-10}\ M_{\odot}\ {\rm yr}^{-1}$, which lies above the (irradiated He disc) instability threshold for orbital periods shorter than ~25 min (Lasota et al. 2008). In addition, considering evolutionary tracks for donor stars in ultra-compact binaries, the above mass accretion rate translates into an orbital period of ~20 min for a He white dwarf donor (Deloye & Bildsten 2003; Sengar et al. 2017). Using the same approach the orbital period would become $\gtrsim$35 min for a He star companion. However, the latter longer orbital period would imply a transient behaviour according to the instability model for He discs (Heinke et al. 2013; Hameury & Lasota 2016).

It should be noted, however, that in some cases it is difficult to reconcile all the observables into a unified picture. For instance, the intermediate thermonuclear bursts displayed by 4U 0614+091 suggest a He-rich companion star, while its optical spectrum points to a C−O rich accretion disc (Kuulkers et al. 2010). Likewise, a He-rich companion was proposed for the ultra-compact 2S 0918−549 based on the detection of intermediate bursts (in 't Zand et al. 2005), while the disc instability models favours a C−O white dwarf companion in order to account for its persistently low luminosity (Heinke et al. 2013). Spallation reactions (Bildsten et al. 1992) have been invoked as a possible solution for this problem (Juett & Chakrabarty 2003; Nelemans et al. 2004). However, this scenario presents several caveats as discussed in in 't Zand et al. (2005), Heinke et al. (2013).

5. Conclusions

We have presented optical (GTC-10.4 m) spectroscopy and Hα imaging of the X-ray binary 4U 1812−12, which is found to be located in the background of the H II region Sharpless 54. The source spectrum is featureless, not showing any of the emission lines typically displayed by LMXBs with H-rich companion stars. In particular, the absence of Hα emission strongly suggests an evolved donor star. We conclude that the lack of H features reported here, together with the persistently dim luminosity and low optical–to–X-ray flux ratio, strongly endorse the ultra-compact nature of 4U 1812−12. We suggest that the companions star is He rich, based on the optical spectrum and the short thermonuclear type I bursts displayed by the system.

Acknowledgements. We acknowledge support from the State Research Agency (AEI) of the Spanish Ministry of Science, Innovation and Universities (MCIU) and the European Regional Development Fund (FEDER) under grant AYA2017-83216-P and AYA2017-83383-P. TMD and MAPT acknowledges support via a Ramón y Cajal Fellowship (RYC-2015-18148 and RYC-2015-17854, respectively). JAFO acknowledges financial support by the Agenzia Spaziale Italiana (ASI) under the research contract 2018-31-HH.0. JG-R acknowledges support from an Advanced Fellowship from the Severo Ochoa excellence program (SEV-2015-0548). JG-R also acknowledges support under grant P/308614 financed by funds transferred from the Spanish Ministry of Science, Innovation and Universities, charged to the General State Budgets and with funds transferred from the General Budgets of the Autonomous Community of the Canary Islands by the MCIU. ND is supported by a Vidi grant from the Netherlands Organisation for Scientific Research (NWO). Based on observations made with the Gran Telescopio Canarias (GTC), installed in the Spanish Observatorio del Roque de los Muchachos of the Instituto de Astrofísica de Canarias, in the island of La Palma, under Director's Discretionary Time and Committee Allocation Time. This work is partly based on data obtained with the SHARDS filter set, purchased by Universidad Complutense de Madrid (UCM). SHARDS was funded by the Spanish Government through grant AYA2012-31277. MOLLY software developed by T.R. Marsh is gratefully acknowledged.

References

Armas Padilla, M., & López-Navas, E. 2019, MNRAS, 488, 5014
Baglio, M. C., Mainetti, D., D'Avanzo, P., et al. 2014, A&A, 572, A99
Baglio, M. C., D'Avanzo, P., Campana, S., et al. 2016, A&A, 587, A102
Barret, D., Olive, J. F., & Oosterbroek, T. 2003, A&A, 400, 643
Bassa, C. G., Jonker, P. G., in 't Zand, J. J. M., & Verbunt, F. 2006, A&A, 446, L17
Bildsten, L., Salpeter, E. E., & Wasserman, I. 1992, ApJ, 384, 143
Bradley, L., Sipocz, B., Robitaille, T., et al. 2019, https://doi.org/10.5281/zenodo.2533376

[3] We assumed an average 2−10 keV continuum X-ray unabsorbed flux of 3.8×10^{-10} erg cm^{-2} s^{-1} (Cocchi et al. 2000), a bolometric correction of 2.9 (in 't Zand et al. 2007), and a distance of 4.6 kpc for which an accretion of helium-rich material was assumed (Jonker & Nelemans 2004).

Casares, J. 2015, ApJ, 808, 80
Casares, J., Jonker, P. G., & Israelian, G. 2017, Handbook of Supernovae (Springer International Publishing), 1499
Cepa, J., Aguiar-Gonzalez, M., Gonzalez-Escalera, V., et al. 2000, Proc. SPIE, 4008, 623
Chambers, K. C., Magnier, E. A., Metcalfe, N., et al. 2016, ArXiv e-prints [arXiv:1612.05560]
Charles, P. A., & Coe, M. J. 2006, in Compact Stellar X-ray Sources, eds. W. Lewin, & M. van der Klis (Cambridge: Cambridge University Press), 39, 690
Cocchi, M., Bazzano, A., Natalucci, L., et al. 2000, A&A, 357, 527
Cooke, R., Kuncic, Z., Sharp, R., & Bland-Hawthorn, J. 2007, ApJ, 667, L163
Cooke, R., Bland-Hawthorn, J., Sharp, R., & Kuncic, Z. 2008, ApJ, 687, L29
Coriat, M., Fender, R. P., & Dubus, G. 2012, MNRAS, 424, 1991
Craig, M., Crawford, S., Seifert, M., Robitaille, T., & Sipocz, B. 2017, https://doi.org/10.5281/zenodo.1069648
Cumming, A. 2003, ApJ, 595, 1077
Degenaar, N., Altamirano, D., Parker, M., et al. 2016, MNRAS, 461, 4049
Deloye, C. J., & Bildsten, L. 2003, ApJ, 598, 1217
Falanga, M., Chenevez, J., Cumming, A., et al. 2008, A&A, 484, 43
Fender, R. P., Russell, D. M., Knigge, C., et al. 2009, MNRAS, 393, 1608
Forman, W., Tananbaum, H., & Jones, C. 1976, ApJ, 206, L29
Galloway, D. K., Muno, M. P., Hartman, J. M., Psaltis, D., & Chakrabarty, D. 2008, ApJS, 179, 360
Galloway, D. K., Yao, Y., Marshall, H., Misanovic, Z., & Weinberg, N. 2010, ApJ, 724, 417
Galloway, D. K., in 't Zand, J., Chenevez, J., et al. 2020, ApJS, 249, 32
Hameury, J.-M., & Lasota, J.-P. 2016, A&A, 594, A87
Heinke, C. O., Ivanova, N., Engel, M. C., et al. 2013, ApJ, 768, 184
Hernández Santisteban, J. V., Cúneo, V., Degenaar, N., et al. 2019, MNRAS, 488, 4596
Homer, L., Anderson, S. F., Wachter, S., & Margon, B. 2002, AJ, 124, 3348
in 't Zand, J. J. M., Cumming, A., van der Sluys, M. V., Verbunt, F., & Pols, O. R. 2005, A&A, 441, 675
in 't Zand, J. J. M., Jonker, P. G., & Markwardt, C. B. 2007, A&A, 465, 953
in 't Zand, J. J. M., Bassa, C. G., Jonker, P. G., et al. 2008, A&A, 485, 183
Jonker, P. G., & Nelemans, G. 2004, MNRAS, 354, 355
Juett, A. M. M., & Chakrabarty, D. 2003, ApJ, 599, 498
Kuulkers, E., in 't Zand, J. J. M., Atteia, J. L., et al. 2010, A&A, 514, A65
Lasota, J.-P. 2001, MNRAS, 45, 449
Lasota, J. P., Dubus, G., & Kruk, K. 2008, A&A, 486, 523
Magrini, L., Perinotto, M., Corradi, R. L., & Mampaso, A. 2003, A&A, 400, 511
Mata Sánchez, D., Muñoz-Darias, T., Casares, J., et al. 2018, MNRAS, 481, 2646
Muno, M. P., Pfahl, E., Baganoff, F. K., et al. 2005, ApJ, 622, L113
Murakami, T., Inoue, H., Koyama, K., et al. 1983, PASJ, 35, 537
Nelemans, G., & Jonker, P. G. 2010, New Astron. Rev., 54, 87
Nelemans, G., Jonker, P. G., Marsh, T. R., & Van Der Klis, M. 2004, MNRAS, 348, L7
Nelemans, G., Jonker, P. G., & Steeghs, D. 2006, MNRAS, 370, 255
Nelemans, G., Wood, M., Groot, P., et al. 2009, Astro2010: The Astronomy and Astrophysics Decadal Survey, Science White Papers, 221
Öttl, S., Kimeswenger, S., & Zijlstra, A. A. 2014, A&A, 565, A87
Predehl, P., & Schmitt, J. 1995, A&A, 293, 889
Price-Whelan, A. M., Sipőcz, B. M., Günther, H. M., et al. 2018, AJ, 156, 123
Rappaport, S., Joss, P. C., & Webbink, R. F. 1982, ApJ, 254, 616
Revnivtsev, M. G., Zolotukhin, I. Y., & Meshcheryakov, A. V. 2012, MNRAS, 421, 2846
Robitaille, T. P., Tollerud, E. J., Greenfield, P., et al. 2013, A&A, 558, A33
Russell, D. M., Fender, R. P., Gallo, E., & Kaiser, C. R. 2007, MNRAS, 376, 1341
Sabbadin, F., & D'Odorico, S. 1976, A&A, 49, 119
Schulz, N. S., Chakrabarty, D., Marshall, H. L., et al. 2001, ApJ, 563, 941
Sengar, R., Tauris, T. M., Langer, N., & Istrate, A. G. 2017, MNRAS, 470, L6
Strohmayer, T. E., Arzoumanian, Z., Bogdanov, S., et al. 2018, ApJ, 858, L13
Tarana, A., Bazzano, A., Ubertini, P., et al. 2006, A&A, 448, 335
Tauris, T. M. 2018, Phys. Rev. Lett., 121, 131105
Tudor, V., Miller-Jones, J. C. A., Knigge, C., et al. 2018, MNRAS, 476, 1889
Van Haaften, L. M., Nelemans, G., Voss, R., et al. 2013, A&A, 552, A69
van Paradijs, J., & McClintock, J. 1994, A&A, 290, 133
Warwick, R. S., Marshall, N., Fraser, G. W., et al. 1981, MNRAS, 197, 865
Werner, K., Nagel, T., Rauch, T., Hammer, N. J., & Dreizler, S. 2006, A&A, 450, 725
Wiersema, K., Russell, D. M., Degenaar, N., et al. 2009, MNRAS, 397, L6
Wilson, C. A., Patel, S. K., Kouveliotou, C., et al. 2003, ApJ, 596, 1220
Yuan, H. B., Liu, X. W., & Xiang, M. S. 2013, MNRAS, 430, 2188
Zhong, J., & Wang, Z. 2011, ApJ, 729, 8
Zucker, C., Speagle, J. S., Schlafly, E. F., et al. 2020, A&A, 633, A51